Preprints.org

Article

Not peer-reviewed version

Antibacterial Thermo-Sensitive Silver Hydrogel Nanocomposite Improves Wound Healing

Nafise Amiri , Sahand Ghaffari , Ida Hassanpour , Taesik Chae , Reza Jalili , Ruhangiz Kilani , Frank Ko , Aziz Ghahary , Dirk Lange *

Posted Date: 5 June 2023

doi: 10.20944/preprints202306.0308.v1

Keywords: Wound healing; Antibacterial; Hydrogel; Meshfill; Silver nanocomposite

Preprints.org is a free multidiscipline platform providing preprint service that is dedicated to making early versions of research outputs permanently available and citable. Preprints posted at Preprints.org appear in Web of Science, Crossref, Google Scholar, Scilit, Europe PMC.

Copyright: This is an open access article distributed under the Creative Commons Attribution License which permits unrestricted use, distribution, and reproduction in any medium, provided the original work is properly cited.

Preprints (www.preprints.org) | NOT PEER-REVIEWED | Posted: 5 June 2023 doi:10.20944/preprints202306.0308.v1

Disclaimer/Publisher's Note: The statements, opinions, and data contained in all publications are solely those of the individual author(s) and contributor(s) and not of MDPI and/or the editor(s). MDPI and/or the editor(s) disclaim responsibility for any injury to people or property resulting from any ideas, methods, instructions, or products referred to in the content.

Article

Antibacterial Thermo-Sensitive Silver Hydrogel Nanocomposite Improves Wound Healing

Nafise Amiri [1,2], Sahand Ghaffari [3], Ida Hassanpour [1], Taesik Chae [4], Reza Jalili [5], Ruhangiz Kilani [1,#], Frank Ko [4], Aziz Ghahary [1,#] and Dirk Lange [3,*]

[1] Professional Fire Fighters' Burn and Wound Healing Research Laboratory, Division of Plastic Surgery, Department of Surgery, University of British Columbia, Vancouver, Canada
[2] ICORD and Department of Pathology & Laboratory Medicine, University of British Columbia, Vancouver, Canada
[3] The Stone Centre at Vancouver General Hospital, Department of Urologic Sciences, University of British Columbia, Vancouver, Canada
[4] Department of Materials Engineering, University of British Columbia, Vancouver, Canada
[5] Aspect Biosystems, Vancouver, Canada
* Correspondence: dirk.lange@ubc.ca
[#] Retired.

Abstract: Introduction: Among the many factors that may limit effective wound healing in patients with chronic ulcers, bacterial infection and poor cell recruitment are primary causes that contribute to prolonged healing. Thus, a novel strategy that aims to prevent bacterial infection within the wound, while at the same time providing structural scaffolding that promotes endogenous tissue repair, would be of great interest. Here, we developed a thermo-sensitive silver nanoparticle hydrogel composite as an antibacterial nutritional scaffold for the wound that contains all nutrients required for cell growth while preventing bacterial infection with the ability to fill up all the cavities and void areas in wounds regardless of their geometry. Methods: Silver nanoparticles (AgNPs) were synthesized by chemical reduction. After characterization, silver hydrogel nanocomposite was developed by reconstitution of collagen-based hydrogel powder in a nanoparticle suspension of varying AgNPs concentrations (200, 400, and 600 ppm). The antibacterial activity of the formulations was examined in vitro and in vivo in subcutaneous implant infected model. The wound healing efficacy of the hydrogel nanocomposite was also evaluated using a splinted wound model in rats through comparison of clinical wound measurements and histological assessments. Cytocompatibility assay and biochemical analysis of blood at the end of in vivo wound healing study were performed to evaluate the safety of formulations. Results: The synthesized nanoparticles were spherical and stable. While hydrogel alone did not show any bacterial reduction in vitro, the inhibition of bacterial growth was significant in all silver hydrogel nanocomposites compared to controls ($p < 0.05$) and was dose-dependent, with maximum reduction observed in the 600 ppm group (4.56±0.26 LOG CFU/mL, $P<0.001$). All concentrations of AgNPs hydrogel composites showed significant antibacterial activity in vivo as well ($P<0.0001$). Treatment of splinted wounds with AgNPs hydrogel composite resulted in faster wound closure and accelerated wound re-epithelialization. The formulations were non-cytotoxic and did not differ significantly in hematological and biochemical factors from the control group in in vivo study. Conclusions: By presenting promising antibacterial and wound healing activity, silver hydrogel nanocomposite offers a safe therapeutic option that can be used as a functional scaffold for an acceleration of wound healing.

Keywords: wound healing; antibacterial; hydrogel; meshfill; silver nanocomposite

1. Introduction

Chronic wounds affect millions of patients all around the world and contribute significantly to their morbidity and mortality [1–3]. Among the many factors that may limit effective wound healing in patients with chronic wounds, bacterial infection and biofilm formation, and poor cell recruitment are primary causes that contribute to prolonged healing [3–7]. Therefore, a strategy that aims to

© 2023 by the author(s). Distributed under a Creative Commons CC BY license.

Preprints (www.preprints.org) | NOT PEER-REVIEWED | Posted: 5 June 2023 doi:10.20944/preprints202306.0308.v1

prevent bacterial infection within the wound, while simultaneously providing structural scaffolding that promotes endogenous tissue repair, would be of great interest.

Hydrogels are promising candidates for wound dressings due to their extraordinary properties. The high water content and their ability to keep the wound environment moist is proven to facilitate healing [8]. In addition to their inherent properties, other functional aspect such as enhanced cell attachment, angiogenesis, and antibacterial activity could be integrated to hydrogels to provide superior functionality for treatment of chronic wounds [9]. A number of natural and synthetic polymeric materials are in use to produce hydrogel dressings. Our group has previously reported the injectable hydrogel composed of cross-linked bovine collagen type I and chondroitin sulfate, supplemented with polyvinyl alcohol (PVA), and it contains optimum concentration of necessary amino acids, vitamins, and minerals required for cell growth and proliferation [10].

We have previously examined the physical characteristics of our scaffold, including its tensile strength, fibril formation, thermal stability, collagenase digestion, and demonstrated maintained cell viability and morphology in vitro [11–13]. We have also shown that the topical application of our injectable scaffold in open wounds in a mouse model improves the healing outcome [11,14]. To improve the current product to enable it to manage infection and protect wounds from bacterial contamination, we used silver nanoparticles (AgNPs) to add antibacterial activity to the hydrogel. We show that this Ag hydrogel nanocomposite could provide a moist and balanced wound environment while protecting it from external contamination. The antimicrobial activity of silver has been known for many years, and literature shows that silver-based therapies have been used in wound care management for a long time. However, these therapies are associated with certain limitations such as toxicity, skin discoloration, and bacterial resistance which have limited their use [15,16]. AgNPs have shown the potential to circumvent these limitations and have gained considerable attention in wound bioburden reduction and in anti-inflammation, as they can release Ag^{+} ions at a greater rate than bulk silver, by virtue of their large specific surface area [17,18].

In this study, we developed a new Ag hydrogel nanocomposite, initially synthesizing it using two non-toxic reducing agents. After full characterization, we reconstituted freeze-dried collagen-GAG hydrogel in synthesized AgNPs colloidal solution with different concentrations of silver to prepare Ag hydrogel nanocomposite. The Ag hydrogel nanocomposite exhibited very effective bactericidal activity against both Gram-negative and Gram-positive bacteria while not showing any cytotoxicity. Furthermore, accelerated wound closure and faster re-epithelialization were observed when we evaluated the efficacy and safety of our Ag hydrogel nanocomposite in an animal model.

2. Results and discussion

Bacterial infection and poor cell recruitment are two primary factors that can significantly impede the process of wound healing in patients with chronic ulcers. As a result, finding innovative approaches that effectively address these issues and simultaneously facilitate endogenous tissue repair through structural scaffolding holds immense promise. Such a novel strategy would not only prevent bacterial infection within the wound but also promote the natural healing process, leading to expedited and improved wound healing outcomes. Previously, we developed a thermo-sensitive collagen-GAG based hydrogel that is liquid at low temperatures (<4°C), solidifies within 10 to 20 minutes of application to the wound sites, and contains all the amino acids, vitamins and minerals required for cell growth. Being in a liquid form when applied to the wound, it fills up all the cavities and void areas seen in many different skin defects, injuries, and non-healing wounds. To improve the current product such that it would be able to manage infection and protect wounds from bacterial contamination, we used AgNPs to add antibacterial activity to the hydrogel. For this purpose, first we synthesized and characterized AgNPs. Next, lyophilized collagen-GAG hydrogel powder was reconstituted in AgNPs colloidal solution with different concentrations of AgNPs up to 600 ppm to form Ag hydrogel nanocomposite.

AgNPs were synthesized by chemical reduction method and then characterized. The synthetic pathway involved using two new reducing agents that are safe and non-toxic, which allowed for the synthesis of Ag nanoparticles with narrow and unimodal size distribution.

Preprints (www.preprints.org) | NOT PEER-REVIEWED | Posted: 5 June 2023 doi:10.20944/preprints202306.0308.v1

Physicochemical properties of AgNPs are key factors in antibacterial activity and toxicity. We used Dynamic Light Scattering (DLS) and Transmission Electron Microscopy (TEM) to measure size, dispersity and zeta potential of nanoparticles. The TEM images showed nanoparticles had a spherical shape with an average diameter of 23.34±4.37 nm (Figure 1a,b). DLS identified nanoparticles with hydrodynamic diameter in the range of 31.17±0.20 nm (Supplementary Data-S1) and zeta potential of -28.10±1.44 mV which indicated good physical stability of the dispersion due to electrostatic repulsion of individual particles. DLS was also used to evaluate the uniformity of nanoparticle dispersion by measuring Poly Dispersity Index (PDI). The PDI values below 0.2 indicate a narrow size distribution [19]. Here, the PDI of 0.192±0.001 (Supplementary Data S1) shows a narrow unimodal distribution in size for the synthesized silver nanoparticles.

These results were further confirmed by UV-vis spectroscopy which is the most widely used technique for structural characterization of AgNPs. The optical properties of spherical AgNPs are highly dependent on nanoparticle diameter and change when particles aggregate. The absorption spectrum of AgNPs solution immediately after synthesis displayed a symmetrical strong absorption peak, associated with the Surface Plasmon Resonance (SPR), at 410 nm. This finding is consistent with the previous studies, showing that the SPR peak for the spherical AgNPs normally appears between 410 and 480 nm. In addition, the absence of any additional peak and the symmetrical shape of the plasmon band were a good indicator of its monodispersity. As for stability assessment over time, the same characteristic absorption band was detected during 6-month storage at 4 ^{0}C (Figure 1c) displaying the high dispersion stability of AgNPs solution despite long storage.

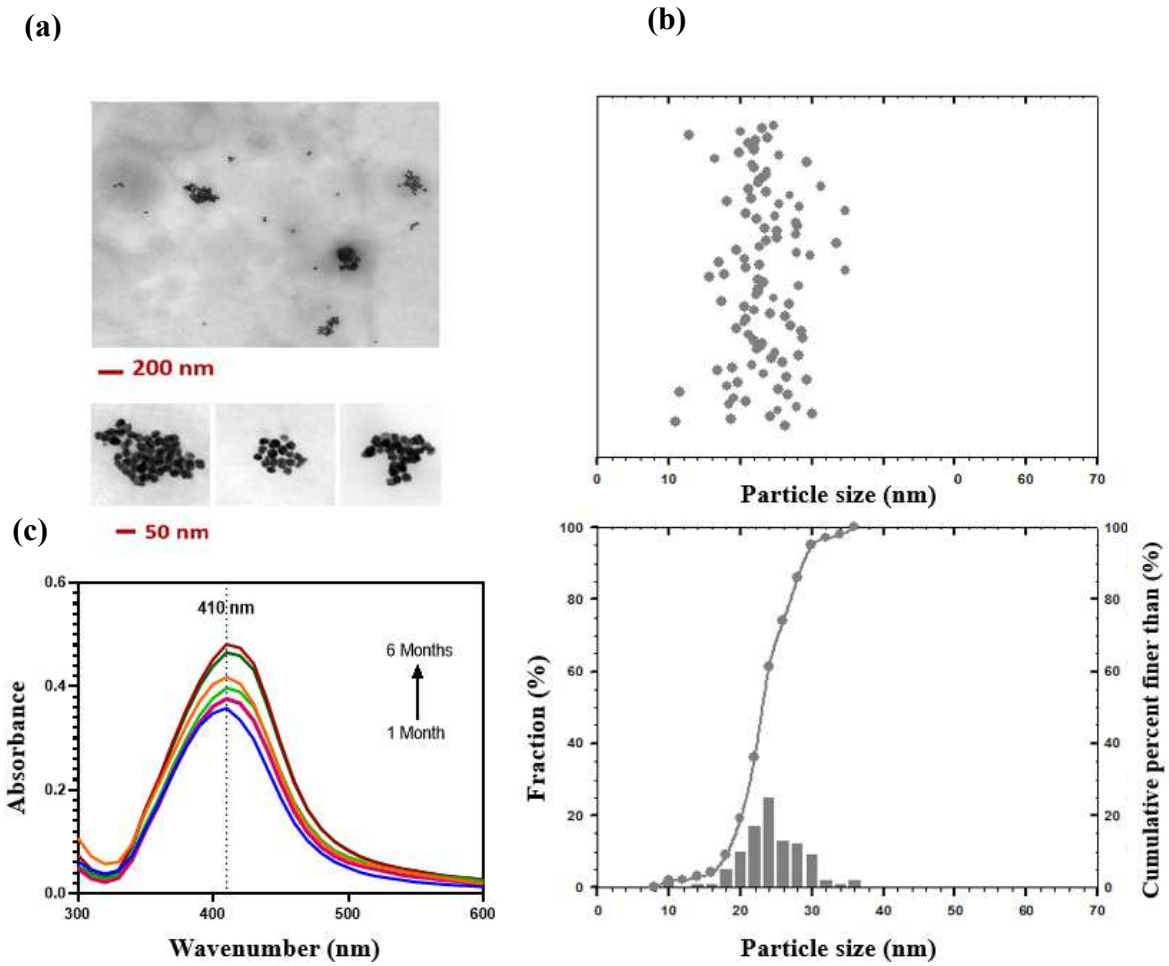

Figure 1. Characterization of synthesized silver nanoparticles. a) TEM images b) Particle size distribution processed by ImageJ c) UV-visible absorption spectra of synthesized silver nanoparticles after storage at 4°C for 6 months, showing a stable absorption band at 410 nm for 6 months.

Preprints (www.preprints.org) | NOT PEER-REVIEWED | Posted: 5 June 2023 doi:10.20944/preprints202306.0308.v1

The *in vitro* toxicity of AgNPs has been evaluated in a wide range of studies and high variation of toxicity has been reported. The main reason for this variation is that the toxicity of AgNPs highly depends on their size and shape. Generally, compared to silver ions, AgNPs show less toxicity both on human dermal fibroblasts and human dermal [20]keratinocytes [20]. When investigating the interaction of human dermal fibroblasts with AgNPs of different sizes, Avalos et al showed smaller particles were much more toxic than the larger AgNPs [21]. In our study the MTT assay on human dermal fibroblast cultured with different concentrations of AgNPs solution showed dose dependent toxicity with an IC50 value of 64 ppm (Figure 2a). This result was very close to results obtained by other investigators for AgNPs of similar size [22,23]. Furthermore, we applied the ISO standard method to investigate the cytocompatibility of the formulation [24]. Interestingly, when combining two systems consisting of AgNPs and collagen hydrogel, the resulting nanocomposite did not have cytotoxic effects (Figure 2b). Both hydrogel alone and Ag hydrogel nanocomposite groups showed high cell viability (>80%), suggesting that the formulations are biocompatible. These results suggest that the hydrogel controls the release of AgNPs, minimizing the cytotoxic effect on the cells. These findings support the potential application of Ag hydrogel nanocomposites as hydrogel dressings for wound management.

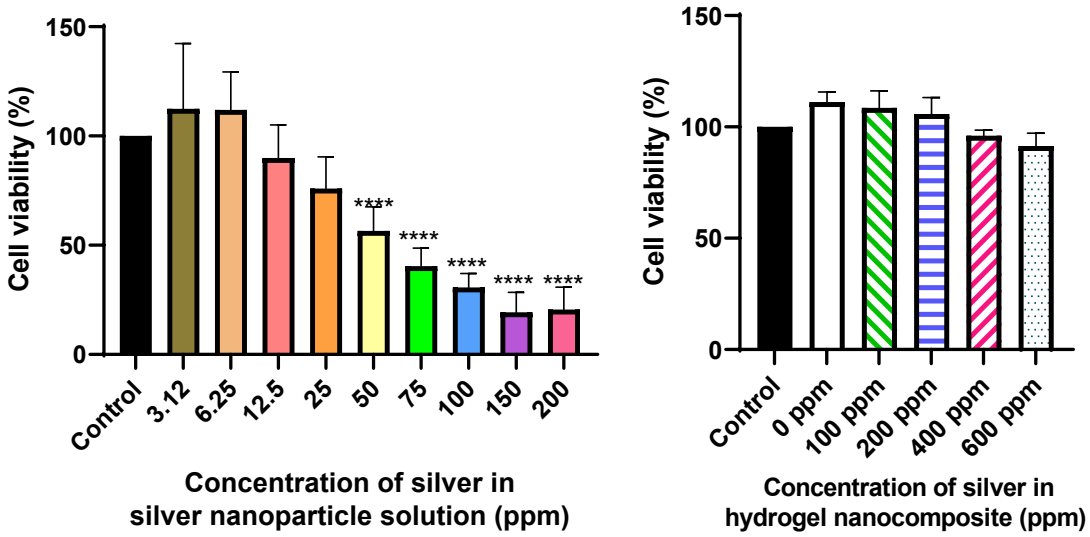

Figure 2. Cytotoxicity. a) Cell Viability (%) of human dermal fibroblast cells incubated in direct contact with MeshFill alone and loaded with different concentrations of AgNPs (50, 100, and 200 ppm) b) Cell Viability (%) of human dermal fibroblast cells incubated with an extract of Ag hydrogel nanocomposite with different concentrations of silver (0, 100, 200, 400 and 600 ppm). The cytotoxicity was evaluated based on the International Organization for Standardization 109993-5 (***P < 0.001).

AgNPs have broad-spectrum antibacterial activity against different bacterial species including Methicillin-Resistant *Staphylococcus aureus* (MRSA) and *Pseudomonas aeruginosa* (PA) which are the most common bacterial species responsible for wound infections. The possible mechanism of the AgNPs antibacterial activity is attributable to a combined effect of both AgNPs and Ag ions including attachment and disruption of the bacterial membrane, damage of intracellular biomolecules and structures, and theinduction of oxidative stress with generation of reactive oxygen species (ROS) and free radicals [25].

In our study, the MICs of AgNPs against MRSA and PA were found to be 79.18 μg/mL and 6.29 ±0.690 μg/mL, respectively. These may be different from values reported in the literature, mainly due to differences in the specific bacterial strains used in a given study. In addition, a direct comparison is not possible as characteristics specific to the AgNP used in a given study that impact activity may differ, including variation in the particle's physicochemical properties such as size, shape, crystallinity, surface chemistry and capping agent [26]. While smaller particles exhibited stronger

Preprints (www.preprints.org) | NOT PEER-REVIEWED | Posted: 5 June 2023 doi:10.20944/preprints202306.0308.v1

antibacterial efficacy compared to those with larger sizes, 20 nm AgNPs showed an MIC of 90 μg/mL against *S. aureus*, while that for *PA* was closer to those reported earlier [27–29] . Similar to our observation, the efficacy of AgNPs of a given size differs between Gram-positive versus Gram-negative bacteria, as indicated by varying MIC values. Interestingly Gram-positive bacteria such as *S. aureus* are more resistant to AgNPs compared to Gram-negative bacteria such as *P. aeruginosa* which may be the result of differences in the overall composition between these bacterial groups, resulting in differences in overall thickness and outer membrane surface charges [30,31]. For instance, Gram-negative bacterial species have a thinner peptidoglycan layer, resulting in easier penetration of AgNPs into these bacteria and greater susceptibility [32].

Given that the AgNPs need to retain their activity when incorporated into the ac tual hydrogel, we verified the antibacterial activity of the Ag hydrogel nanocomposite was against *MRSA* and *PA*. As shown in Figure 3a, exposure of bacteria to hydrogel alone did not result in a reduction in bacterial numbers while exposure to all Ag-containing hydrogels significantly inhibited bacterial growth in a dose-dependent fashion. In Ag hydrogel nanocomposite groups, the drop in the number of bacteria increased with increasing Ag concentration and maximum reduction was observed for the 600 ppm group against both pathogens which resulted in a 4.20±0.33 LOG reduction in *PA* compared to only 1.71±0.35 for the 100 ppm sample. Similarly, the LOG reduction against MRSA was 4.56±0.26 for the 600 ppm sample compared to 2.04±0.69 for the 100 ppm sample.

To assess efficacy of the cast formulations in a more realistic environment, we determined the antimicrobial activity of the cast formulations in a subcutaneous implant infection model. For this, the cast formulations were implanted into subcutaneous pockets on the backs of Sprague-Dawley rats followed by the addition of *MRSA* (10^6 CFU/mL) prior to suturing the implantation site to induce an infection (Figure 3d). Overall, we found a significant reduction in bacterial numbers on day-4 post-infection in the infected pockets containing Ag-hydrogel samples compared to those that only contained hydrogel samples (Figure 3c).

Next, we assessed the potential for the hydrogel to prevent the colonization of a substrate surface that is encased by the hydrogel itself, as this most closely mimics the scenario where a hydrogel treated wurface may be challenged with a higher load of contaminatin bacteria. For this, we cast Ti discs inside hydrogel or Ag-hydrogel and exposed them to a suspension containing 10^6 *MRSA.* The hydrogel or Ag-hydrogel containing the Ti discs was then implanted into subcutaneous pockets of rats as described above and the animals were recovered for 4 days. Overall, Ag-hydrogel was found to significantly reduce the bacterial penetration through the hydrogel and onto the Ti disc surface compared to Ti discs encased in hydrogel only or without hydrogel. The greatest reduction (LOG 6.43±0.38) was found with Ag-hydrogel containing 600 ppm Ag which completely prevented the colonization of the underlying Ti discs with *MRSA*.

Interestingly, while the MIC of AgNPs was lower for *PA*, AgNPs hydrogel composite showed better antibacterial activity against *MRSA* in the penetration test. This could be because *PA* is capable of two distinct types of surface-specific motilities, twitching and swarming [33].

Preprints (www.preprints.org) | NOT PEER-REVIEWED | Posted: 5 June 2023 doi:10.20944/preprints202306.0308.v1

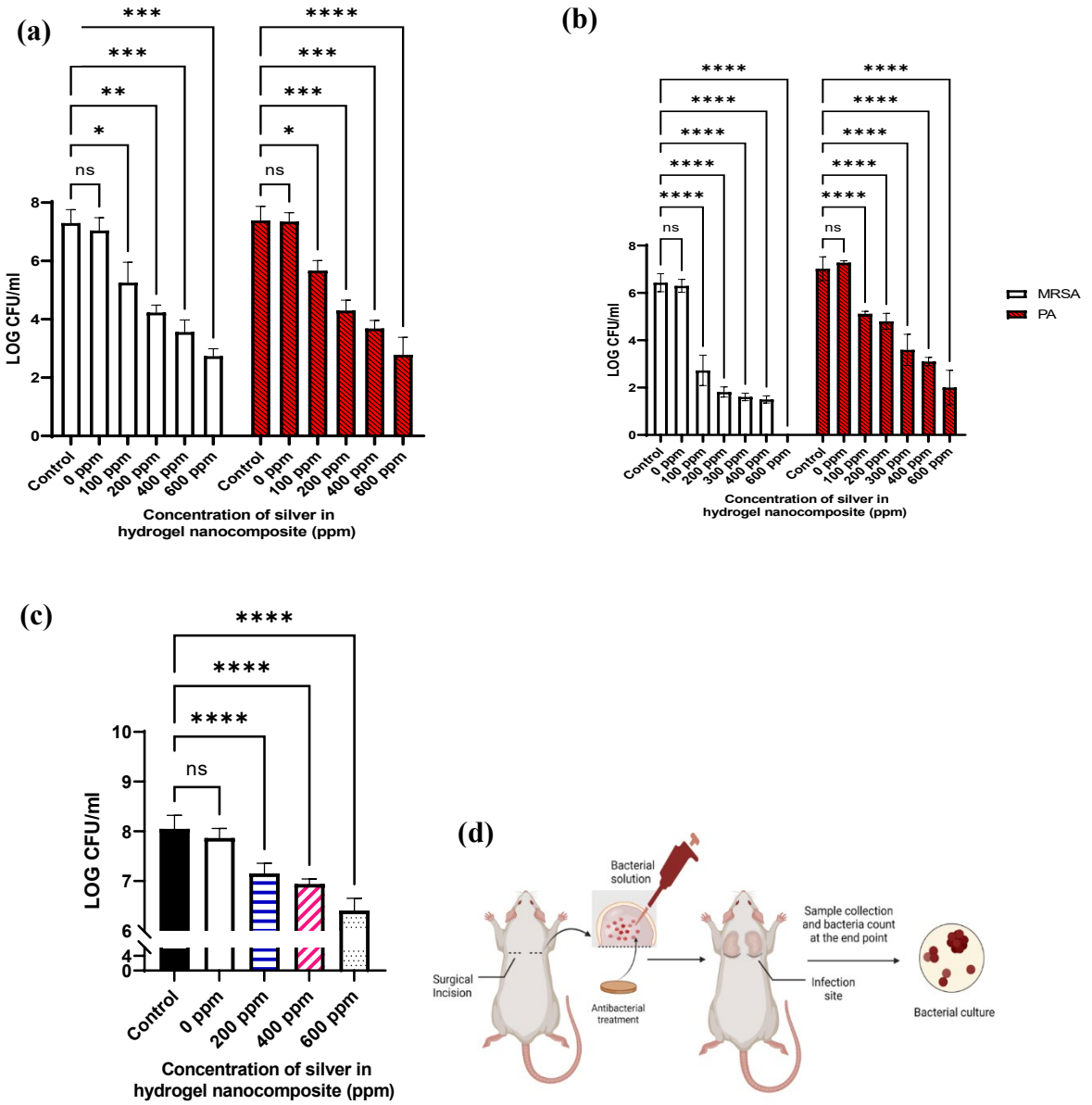

Figure 3. Antibacterial activity. a) Ag hydrogel nanocomposite with different concentrations of AgNPs (0, 100, 200, 400 and 600 ppm) was placed in bacterial solution to be in direct contact with two common wound infecting bacteria; *Methicillin-resistant Staphylococcus aureus* (*MRSA*) (gram-positive) and *Pseudomonas aeruginosa* (*PA*) (gram-negative). After 24h, small aliquots of the bacterial solution were removed and microorganisms in it were enumerated. Bacterial solution alone was considered as a control. In control and hydrogel alone (0 ppm) the significant increase in the number of bacteria was observed in solution after 24h, while AgNPs significantly inhibited the growth of bacteria in Ag hydrogel nanocomposite groups b) The effect of Ag hydrogel nanocomposites in preventing bacteria penetration into the hydrogel. Sterile Titanium (Ti) wire disc was cast inside the hydrogels. The samples were placed in bacterial solution to be in direct contact with two common wound infecting bacteria. After 24h, Ti disc was harvested from inside of the hydrogels and microorganisms on the surface was enumerated. Ti disc alone in bacterial solution was considered as a control. After 24h, all Ag hydrogel nanocomposite groups significantly inhibited penetration of bacteria inside the gel and growth of bacteria on Ti wire surface c) *In vivo* antibacterial activity. Antibacterial activity of formulations was evaluated in subcutaneous infected wound on the dorsal area of rat against *Methicillin-resistant Staphylococcus aureus* (*MRSA*). While there was not any difference between

Preprints (www.preprints.org) | NOT PEER-REVIEWED | Posted: 5 June 2023 doi:10.20944/preprints202306.0308.v1

untreated (control) and hydrogel alone (0 ppm), a significant decrease was observed in CFU of bacteria in all Ag hydrogel nanocomposite groups d) Schematic images of *in vivo* antibacterial study. (*p < 0.05, ** P<0.01, *** P<0.001).

These results confirm that in addition to high cytocompatibility, the AgNPs hydrogel composite exhibited strong antibacterial activity. Such behavior has been reported previously in different synthetic and natural polymers including PVA, PVP, gelatin, and alginate used to prepare antimicrobial Ag-hydrogel nanosystems. Travan et al. described synthesis and stabilization of AgNPs in a chitosan-derived polysaccharide solution and studied the cytotoxicity and antibacterial properties in both solution and within a 3D hydrogel structure. Antimicrobial results showed that the nanocomposite system displays a very effective bactericidal activity toward both Gram-positive and Gram-negative bacteria. However, the hydrogel does not show any cytotoxic effect toward three different eukaryotic cell lines including mouse fibroblast-like (NIH-3T3) cells. They suggested that the nanoparticles, immobilized in the hydrogel matrix, can exert their antimicrobial activity by simple contact with the bacterial membrane, while entrapping AgNPs in hydrogel could prevent them from diffusing into the surrounding environment and making them available for cells to be taken up [34].

Chronic non-healing wounds have a significant impact on numerous patients every year, significantly contributing to their morbidity and mortality. Complications and delayed wound healing are often a result of bacterial infection. Thus, wound dressings with advanced antibacterial activity are of great interest within wound care management. Antibiotic-loaded dressing with controlled release activity can provide antibacterial activity while avoiding the exposure of the healing tissue to toxic concentrations of active agent [35].

To assess the effect of Ag-hydrogel on the wound healing process, we utilized the rodent excisional wound healing model. Considering that the rodent skin is mobile, wound closure for the most part takes place via contraction. To overcome this shortcoming, we used an excisional splinting model in rats. In this model, a splinting ring is tightly attached to the skin around the wound to prevent skin contraction, forcing the wound to heal through granulation and re-epithelialization, a process similar to that occurring in humans.

As shown in Figure 4, wounds exposed to all Ag-hydrogel nanocomposite groups consistently closed faster than both hydrogel alone and control groups, and the original wound area in rats treated with Ag-containing group was significantly smaller at weeks 1, 2, and 3 post-wounding (Figure 4-a, b). That said, using a two-way ANOVA, statistically significant differences in the wound healing process were observed in wounds treated with either hydrogel or Ag-Hydrogel nanocomposite groups compared to control. Having confirmed that both hydrogel or Ag-Hydrogel nanocomposite treatments accelerated the wound healing process from clinical observation, we therefore wondered whether they could provide a favorable microenvironment to speed up the restoration of epidermal and dermal architecture. To investigate this, histological analysis was performed to assess the effect of treatments on skin wound healing in the microstructure. The Trichrome staining of wound site harvested at the end of study (week 3) is shown in Figure 5. Compared to control, wound re-epithelialization was remarkably enhanced after treatment with all Ag-Hydrogel nanocomposites. Therefore, the clinical and histological observations of the *in vivo* study revealed accelerated re-epithelization and better wound contraction with AgNP-hydrogel composites. This result was in agreement with other studies evaluating the wound healing efficacy of biomaterials containing AgNPs.

Preprints (www.preprints.org) | NOT PEER-REVIEWED | Posted: 5 June 2023 doi:10.20944/preprints202306.0308.v1

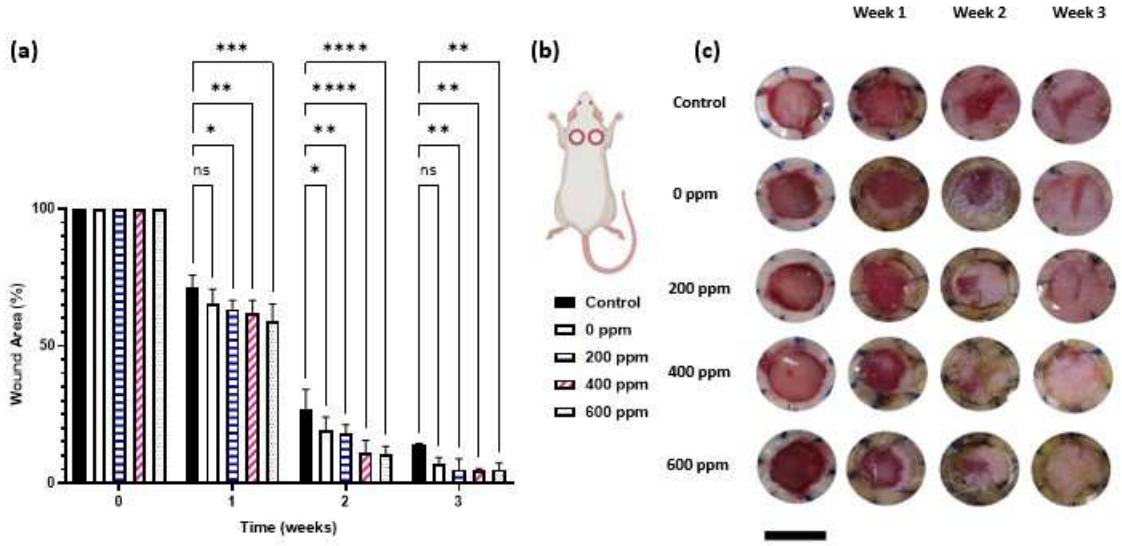

Figure 4. Wound healing study. a) Average wound area measured by Image J® program and plotted as relative % of original wound b) Schematic image of the location of splinted wounds on back of rat c) Representative serial digital images of top view of full-thickness splinted wounds on dorsal region of rats either kept un-treated (control) or treated with silver hydrogel nanocomposites with different concentration of silver (0, 100, 200, 400 and 600 ppm) at week 1, 2, and 3. (*p < 0.05, ** P<0.01, *** P<0.001).

In addition to antibacterial activity, AgNPs play an active role in wound healing. Previous studies have shown that AgNPs promote the migration of fibroblasts and stimulate the differentiation of fibroblasts to myoblasts which speed up the wound contraction and promote the healing process [36]. AgNPs also improve proliferation and migration of keratinocytes from the edge to the center of the wound and trigger the differentiation and maturation of keratinocytes, thus promoting wound contraction [37]. Moreover, the anti-inflammatory property of AgNPs is another mechanism that supports the wound healing process by reducing the level of proinflammatory cytokine or decreasing mast cell infiltration [38].

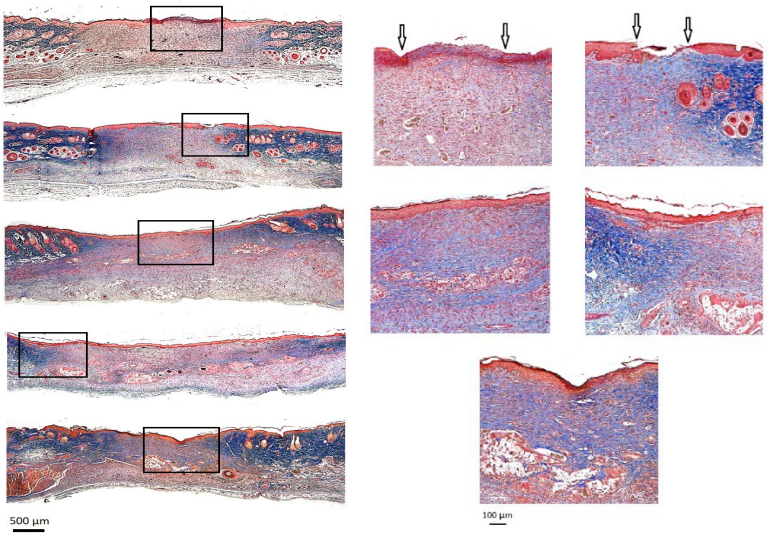

Figure 5. Histological analysis by Masson's Trichrome staining. a) The whole wound at 2x magnification b) The wound at 10x magnification. Black arrows demonstrate incomplete epithelialization.

Preprints (www.preprints.org) | NOT PEER-REVIEWED | Posted: 5 June 2023 doi:10.20944/preprints202306.0308.v1

3. Conclusions

In the present study, we successfully synthesized AgNPs and prepared collagen-based Ag-hydrogel nanocomposites. Our study confirmed that the strategy of using a collagen-based matrix carrying a reservoir of AgNPs in the form of Ag-hydrogel nanocomposite to provide antibacterial activity while accelerating wound healing could have promising outcomes. MIC, *in vitro*, and *in vivo* antimicrobial studies clearly displayed the antibacterial potential of AgNPs and its hydrogel nanocomposites. *In vivo* studies further proved accelerated re-epithelization and better wound healing in wounds treated with Ag-hydrogel nanocomposites. Moreover, no cytotoxic effect was observed when formulations were cultured with human dermal fibroblast and no changes in cell blood count and biochemical parameters of serum were detected in rats at the end of *in vivo* study. Therefore, by presenting favorable antibacterial and wound healing results, Ag-hydrogel nanocomposite offers a safe therapeutic option that can be used as a functional scaffold for acceleration of wound healing.

4. Methods

4.1. Silver nanoparticle synthesis and Ag hydrogel nanocomposite preparation

Silver nanoparticles (AgNPs) were synthesized by chemical reduction method. Silver nitrate ($AgNO_3$) as a source of silver was reduced by trisodium citrate and glucose as reducing agents. A 1 mL volume of 30 mM trisodium citrate was added to 100 mL of distilled deionized water (DDW) under constant stirring and heated up. As the temperature reached 95°C, 2 mL of 5 mM $AgNO_3$ and 50 mM glucose were added to the solution drop by drop. The reaction mixture was stirred vigorously on a magnetic stirrer and heated until the solution color turned light yellow. The resulting AgNPs solution was kept in dark at 4°C for future use. The solution was further centrifuged (10000 rpm for 15 min) and resuspended in DDW to prepare aqueous AgNPs with different concentrations. The colloidal stability and particle size distribution of AgNPs were confirmed before proceeding to Ag hydrogel nanocomposite preparation. Dynamic light scattering (DLS, NanoBrook Omni, Brookhaven instruments, USA) and transmission electron microscopy (TEM, H7600, Hitachi, Japan) were used to assess particle size, morphology, and distribution. The concentration of AgNPs solution was measured by Inductively coupled plasma-mass spectroscopy (ICP-MS). The absorbance spectrum of the colloidal sample was obtained in the range of 300–700 nm, using a UV–Vis spectrometer Shimadzu-UV. The contents, preparation and properties of collagen-GAG hydrogel have been described in detail, previously [10]. To form Ag hydrogel nanocomposite, lyophilized collagen-GAG hydrogel powder was reconstituted in AgNPs aqueous solution with different concentrations.

4.2. In vitro cytocompatibility

4.2.1. Silver nanoparticle cell viability assay

The cytotoxic effect of synthesized silver nanoparticles was measured using MTT assay. Human dermal fibroblasts (HDF) cells were seeded in a 96-well tissue culture plate at a density of 1.5×10^4 cells/well with a pre-warmed fresh medium (DMEM containing 10% fetal bovine serum and 1% penicillin/streptomycin) and incubated at 37 °C in an incubator supplied with 5% CO2 for 24 h. After that, the cells were treated with different concentrations of silver nanoparticles (0, 50, 100, and 200 ppm) and incubated for another 24 h. Next, the test solutions were removed, 100 µL of MTT-containing medium (1 mg/mL) was added to each well and further incubated for 4 h. Then, the supernatants were removed and replaced with 100 µL DMSO to solubilize the resulting purple formazan crystals formed in living cells. The relative cell viability (%) was calculated based on the absorbance at 570 nm measured with a microplate reader (BioTek, USA) according to the following formula:

Cell viability (%) = (optical density of treated cells/ optical density of control cells) × 100

Preprints (www.preprints.org) | NOT PEER-REVIEWED | Posted: 5 June 2023 doi:10.20944/preprints202306.0308.v1

4.2.2. Silver hydrogel nanocomposite cytocompatibility

The cytocompatibility of Ag hydrogel nanocomposite containing different concentrations of AgNPs (0, 100, 200, 400, and 600 ppm) was evaluated based on the International Organization for Standardization 109993-5 using extract analysis. In brief, formulations were extracted in culture medium at 37 °C for 24 h and the extracts were collected for cell culture. Human dermal fibroblasts (HDF) cells were seeded at a density of 1.5×10^4 cells per well of a 96 well plate with a DMEM-high glucose supplemented 10% FBS and a 1% penicillin/streptomycin solution and incubated at 37 °C supplied with 5% CO_2. After 24 h of incubation, the culture medium was removed, each well was washed with phosphate buffered saline (PBS) three times, and then 100 µL of extracts was added per well. Cell proliferation and viability was determined using MTT assay after 24 h of exposure.

4.3. Antibacterial activity

4.3.1. Minimum inhibitory concentration (MIC) of AgNPs solution

A standard broth microdilution method was used to determine the minimal inhibitory concentrations (MIC) of synthesized AgNPs against American type culture collection (ATCC) strains of *Methicillin-resistant Staphylococcus aureus* (MRSA-USA300) (Gram-positive) and *Pseudomonas aeruginosa* (PAO1-#166.lux) (Gram-negative). In brief, a total of eight serially diluted samples were used, starting with a 200 ppm stock solution of AgNPs, 2-fold diluted in ddH_2O (100 µL total volume) seven additional times. The bacterial isolates were cultured and sub-cultured in LB as the growth media under aerobic conditions at 37 ^{0}C, 48 and 24 hours prior to all experiments. A starting colony forming units (CFU) of 10^5 – 10^6 of each bacterial strain was inoculated with the serially diluted AgNPs in 96-well plates and incubated for 24 h. After that, viable counting colonies were enumerated using serial dilution of a 10 µL aliquot from each sample in PBS followed by growth on agar petri dish by incubating for 14-18 h at 37 ^{0}C, according to the following equation:

$$\text{CFU/mL} = [(\#\text{ of countable colonies}) \times (1/\text{dilution factor}) \times 1000\ \mu\text{L/mL}] / (10\ \mu\text{L})$$

4.3.2. Antibacterial activity of Ag hydrogel nanocomposite formulations

Two different methods were applied to evaluate the antibacterial activity of the formulations *in vitro*. In the first method, the disc-shape casted hydrogels were directly placed in bacterial solution to be in direct contact with two common wound infecting bacteria *MRSA* and *PA*. Briefly, 200 µL/well of hydrogel was added to 48–well plate, and kept at room temperature for 10-15min to cast. Then microbial culture containing 10^6 CFU/mL of bacteria was added to the well and then placed in 37^0 C incubator. After 24 h, small aliquots of the bacterial solution were removed and microorganisms in it were enumerated as stated above.

In the second method, the effect of Ag hydrogel nanocomposites in preventing bacteria penetration into the hydrogel was evaluated. To do so, a sterile disc shape Titanium (Ti) wire was placed inside the AgNPs hydrogels prior to casting. Similar to previous method the hydrogel was placed in bacterial solution after casting. The Ti disc was subsequently harvested and number of bacteria infiltrated into the hydrogel and attached to the Ti disc was counted after 24 h incubation at 37^0 C.

4.4. In vivo study

4.4.1. Experimental Animals

Healthy female Sprague Dawley (SD) rats (200 g–300 g, aged 16–24 weeks old) were obtained from Charles River Laboratories. Animal care and all experimental procedures were performed according to the Guide for the Care and Use of Laboratory Animals of the University of British Columbia Animal Care Committee. The clearance to conduct this study was provided by the University of British Columbia Committee of Animals and Ethics (protocol approval ID: A17-0292

Preprints (www.preprints.org) | NOT PEER-REVIEWED | Posted: 5 June 2023 doi:10.20944/preprints202306.0308.v1

for antibacterial study and A18-0366 for wound healing study). The rats were maintained with water and standard laboratory chow ad libitum for 1 week prior to the experiment to acclimatize to the laboratory environment in a temperature-controlled room. The animals were randomly divided into study groups and were individually anesthetized using 2% isoflurane in oxygen (flow rate of 1.0 L/min) and kept under anesthesia throughout the procedure.

4.4.2. In vivo antibacterial study

To determine the efficacy of Ag hydrogel nanocomposite formulations on bacterial growth inhibition in an *in vivo* setting, we used a subcutaneous infection wound model using rats. After fur removal with electric clipper, an 8 mm incision was made on either side of the median line on the dorsal aspect of the animal. A subcutaneous pocket was formed by blunt dissection technique (using a sterile hemostat) large enough to insert a 1 cm x 0.5 cm cast hydrogel that was either bare or loaded with AgNPs. Infection was induced by inoculating 10^6 MRSA inside each pocket. Following implantation, the incisions were closed with absorbable sutures. On day 4 post-surgical implant, animals were sacrificed and the whole pockets and surrounding tissue were harvested. Harvested tissues were then homogenized using a Precellys24 tissue homogenizer and the number of bacteria were quantified by serial dilution in PBS, followed by plating on agar and CFU counting in 14-18 h.

4.4.3. In vivo wound healing study

The rat excisional wound splinting model was used to determine the efficacy of Ag hydrogel nanocomposite in wound healing. Following aseptic surgical techniques, two full-thickness excisional wounds with 8 mm diameter circular wounds were created bilaterally on either side of the vertebral column of each rat. To overcome the problem of wound contracture in rodent wounds, silicone splints with an inner and outer diameter of 10 and 14 mm were secured on the edges of the wound. Five experimental groups were tested with either: 1) clean untreated wounds; 2) clean wounds filled with CG Hydrogel alone; 3,4,5) clean wounds filled with Ag hydrogel nanocomposite containing 200, 400, and 600 ppm of Ag, respectively. The wound healing process was monitored every 3 days for up to 3 weeks.

Wound surface area calculation

Digital images of the wound area were captured on different time points. The images were processed with ImageJ® software (Image J 1.4, NIH, USA) for surface area changes. Total reduction in the wound size was calculated by dividing the surface area at each time point to that of the original wound using the following equation:

$$\text{Total Wound Closure (\%)} = 100 - \left[\frac{\text{Wound surface area}}{\text{Original wound surface area}} \times 100\right]$$

Histological Analysis

At the end point of the study, all wound sites were harvested for histological evaluation. Tissue samples were fixed in 10% neutral buffered formalin solution (Sigma-Aldrich, St. Louis, MO, USA) for 24 h before being processed and embedded in paraffin blocks. Samples were sectioned at 5 µm thickness and stained using Masson's Trichrome stain. Briefly, slides were incubated in Bouin's solution for 1 h at 60° C. Then, rinsing slides were stained with Weigert's Hematoxylin solution (Sigma–Aldrich) followed by Biebrich Scarlet-Acid Fuchsin, phosphomolybdic–phosphotungstic acid, aniline blue, and 1% acetic acid solution. Collagen appears blue, nuclei black, and cytoplasm red.

Hematology analysis and Biochemical assay

To examine the safety and evidence of systemic inflammatory response, blood cell count and biochemical assay were conducted at the end of animal study. Blood samples were obtained by

Preprints (www.preprints.org) | NOT PEER-REVIEWED | Posted: 5 June 2023 doi:10.20944/preprints202306.0308.v1

cardiac puncture. Separate portions of blood were transferred to tubes containing either lithium heparin or trisodium EDTA as anticoagulants. The whole blood was used to count total red blood cells (RBC), white blood cells (WBC), platelets, and hemoglobin (or hematocrit). The blood serum was processed in a VETSCAN Analyzer (Abaxis Inc., US) for analysis of the following parameters: total protein (TP), alkaline phosphatase (ALP), alanine transaminase (ALT), glucose (GLC), blood urea nitrogen (BUN), and creatinine (CR).

4.5. Statistical Analysis

All data were presented as the mean ± standard deviation of three independent experiments. Data were subjected to statistical analysis using paired student's *t*-test, one-way or two-way analysis of variance (ANOVA) with GraphPad Prism 9.0.0 (121) (GraphPad Software Inc., San Diego, CA). Post-hoc test was performed using the Dunnett test. Mean values were considered to be statistically significant at and $P < 0.05$ (*), $P < 0.01$ (**), $P < 0.001$ (***).

Supplementary Materials: The following supporting information can be downloaded at the website of this paper posted on Preprints.org.

Funding: This research was funded by "The Collaborative Health Research Program (CHRP) Sponsored by both the Canadian Institutes of Health Research (CIHR) and Natural Sciences and Engineering Research Council of Canada (NSERC)", grant number CPG-163966.The APC was funded by the British Columbia Burn Fund.

Data Availability Statement: The data that support the findings of this study are available from the corresponding author upon request.

Conflicts of Interest: A.G. is the leading inventor of the liquid scaffold technology involved in this study. The remaining authors declare no conflict of interest. The funders had no role in the design of the study; in the collection, analyses, or interpretation of data; in the writing of the manuscript, or in the decision to publish the results.

References

1. V. Falanga, R.R. Isseroff, A.M. Soulika, M. Romanelli, D. Margolis, S. Kapp, M. Granick, K. Harding, Chronic wounds, Nat Rev Dis Primers. 8 (2022) 50. https://doi.org/10.1038/s41572-022-00377-3.
2. J. Escandon, A.C. Vivas, J. Tang, K.J. Rowland, R.S. Kirsner, High mortality in patients with chronic wounds, Wound Repair and Regeneration. 19 (2011) 526–528. https://doi.org/10.1111/j.1524-475X.2011.00699.x.
3. R.G. Frykberg, J. Banks, Challenges in the Treatment of Chronic Wounds, Adv Wound Care (New Rochelle). 4 (2015) 560–582. https://doi.org/10.1089/wound.2015.0635.
4. S.J.Mohd. Yussof, E. Omar, D.R. Pai, S. Sood, Cellular events and biomarkers of wound healing, Indian Journal of Plastic Surgery. 45 (2012) 220–228. https://doi.org/10.4103/0970-0358.101282.
5. K. Raziyeva, Y. Kim, Z. Zharkinbekov, K. Kassymbek, S. Jimi, A. Saparov, Immunology of Acute and Chronic Wound Healing, Biomolecules. 11 (2021) 700. https://doi.org/10.3390/biom11050700.
6. G. Zhao, M.L. Usui, S.I. Lippman, G.A. James, P.S. Stewart, P. Fleckman, J.E. Olerud, Biofilms and Inflammation in Chronic Wounds, Adv Wound Care (New Rochelle). 2 (2013) 389–399. https://doi.org/10.1089/wound.2012.0381.
7. A. Clinton, T. Carter, Chronic Wound Biofilms: Pathogenesis and Potential Therapies, Lab Med. 46 (2015) 277–284. https://doi.org/10.1309/LMBNSWKUI4JPN7SO.
8. X. Zhang, M. Qin, M. Xu, F. Miao, C. Merzougui, X. Zhang, Y. Wei, W. Chen, D. Huang, The fabrication of antibacterial hydrogels for wound healing, Eur Polym J. 146 (2021) 110268. https://doi.org/10.1016/j.eurpolymj.2021.110268.
9. H. Nosrati, R. Aramideh Khouy, A. Nosrati, M. Khodaei, M. Banitalebi-Dehkordi, K. Ashrafi-Dehkordi, S. Sanami, Z. Alizadeh, Nanocomposite scaffolds for accelerating chronic wound healing by enhancing angiogenesis, J Nanobiotechnology. 19 (2021) 1–21. https://doi.org/10.1186/s12951-020-00755-7.
10. M. (Sam) Pakyari, R.B. Jalili, R.T. Kilani, N. Amiri, E. Brown, A. Ghahary, Studying the in vivo application of a liquid dermal scaffold in promoting wound healing in a mouse model, Exp Dermatol. 31 (2022) 715–724. https://doi.org/10.1111/exd.14504.

Preprints (www.preprints.org) | NOT PEER-REVIEWED | Posted: 5 June 2023 doi:10.20944/preprints202306.0308.v1

11. R. Hartwell, B. Chan, K. Elliott, H. Alnojeidi, A. Ghahary, Polyvinyl alcohol-graft-polyethylene glycol hydrogels improve utility and biofunctionality of injectable collagen biomaterials, Biomedical Materials. 11 (2016) 35013. https://doi.org/10.1088/1748-6041/11/3/035013.
12. R. Hartwell, V. Leung, C. Chavez-Munoz, L. Nabai, H. Yang, F. Ko, A. Ghahary, A novel hydrogel-collagen composite improves functionality of an injectable extracellular matrix, Acta Biomater. 7 (2011) 3060–3069. https://doi.org/10.1016/j.actbio.2011.04.024.
13. R. Hartwell, M.S. Poormasjedi-Meibod, C. Chavez-Munoz, R.B. Jalili, A. Hossenini-Tabatabaei, A. Ghahary, An in-situ forming skin substitute improves healing outcome in a hypertrophic scar model, Tissue Eng Part A. 21 (2015) 1085–1094. https://doi.org/10.1089/ten.tea.2014.0271.
14. M. Verly, E. Mason, S. Sheikh-Oleslami, R. Jalili, B. Russ, R.T. Kilani, A. Ghahary, A Pilot Trial Assessing the Feasibility and Efficacy of a Novel Powder for Rapid Wound Healing, European Burn Journal. 2 (2021) 238–248. https://doi.org/10.3390/ebj2040018.
15. I. Khansa, A.R. Schoenbrunner, C.T. Kraft, J.E. Janis, Silver in Wound Care-Friend or Foe?: A Comprehensive Review., Plast Reconstr Surg Glob Open. 7 (2019) e2390. https://doi.org/10.1097/GOX.0000000000002390.
16. C.A. Lariviere, A.B. Goldin, J. Avansino, Silver toxicity with the use of silver-impregnated dressing and wound vacuum-assisted closure in an immunocompromised patient., J Am Col Certif Wound Spec. 3 (2011) 8–12. https://doi.org/10.1016/j.jcws.2011.05.002.
17. S. Lee, B.-H. Jun, Silver Nanoparticles: Synthesis and Application for Nanomedicine, Int J Mol Sci. 20 (2019) 865. https://doi.org/10.3390/ijms20040865.
18. Y. Qing, L. Cheng, R. Li, G. Liu, Y. Zhang, X. Tang, J. Wang, H. Liu, Y. Qin, Potential antibacterial mechanism of silver nanoparticles and the optimization of orthopedic implants by advanced modification technologies, Int J Nanomedicine. Volume 13 (2018) 3311–3327. https://doi.org/10.2147/IJN.S165125.
19. R. Vazquez-Muñoz, N. Bogdanchikova, A. Huerta-Saquero, Beyond the Nanomaterials Approach: Influence of Culture Conditions on the Stability and Antimicrobial Activity of Silver Nanoparticles., ACS Omega. 5 (2020) 28441–28451. https://doi.org/10.1021/acsomega.0c02007.
20. J. Franková, V. Pivodová, H. Vágnerová, J. Juráňová, J. Ulrichová, Effects of silver nanoparticles on primary cell cultures of fibroblasts and keratinocytes in a wound-healing model, J Appl Biomater Funct Mater. 14 (2016) e137–e142. https://doi.org/10.5301/jabfm.5000268.
21. A. Avalos, A.I. Haza, D. Mateo, P. Morales, Interactions of manufactured silver nanoparticles of different sizes with normal human dermal fibroblasts, Int Wound J. 13 (2016) 101–109. https://doi.org/10.1111/iwj.12244.
22. E. Szczepańska, A. Bielicka-Giełdoń, K. Niska, J. Strankowska, J. Żebrowska, I. Inkielewicz-Stępniak, B. Łubkowska, T. Swebocki, P. Skowron, B. Grobelna, Synthesis of silver nanoparticles in context of their cytotoxicity, antibacterial activities, skin penetration and application in skincare products, Supramol Chem. 32 (2020) 207–221. https://doi.org/10.1080/10610278.2020.1726917.
23. S. Loganathan, K. Selvam, M.S. Shivakumar, S. Senthil-Nathan, P. Vasantha-Srinivasan, D. Gnana Prakash, S. Karthi, F. Al-Misned, S. Mahboob, A. Abdel-Megeed, A. Ghaith, P. Krutmuang, Phytosynthesis of Silver Nanoparticle (AgNPs) Using Aqueous Leaf Extract of Knoxia Sumatrensis (Retz.) DC. and Their Multi-Potent Biological Activity: An Eco-Friendly Approach, Molecules. 27 (2022) 7854. https://doi.org/10.3390/molecules27227854.
24. P. Thangaraju, S.B. Varthya, ISO 10993: Biological Evaluation of Medical Devices, in: Medical Device Guidelines and Regulations Handbook, Springer International Publishing, Cham, 2022: pp. 163–187. https://doi.org/10.1007/978-3-030-91855-2_11.
25. S. Tang, J. Zheng, Antibacterial Activity of Silver Nanoparticles: Structural Effects, Adv Healthc Mater. 7 (2018) 1–10. https://doi.org/10.1002/adhm.201701503.
26. S. Agnihotri, S. Mukherji, S. Mukherji, Size-controlled silver nanoparticles synthesized over the range 5–100 nm using the same protocol and their antibacterial efficacy, RSC Adv. 4 (2014) 3974–3983. https://doi.org/10.1039/C3RA44507K.
27. S. Shah, S. Gaikwad, S. Nagar, S. Kulshrestha, V. Vaidya, N. Nawani, S. Pawar, Biofilm inhibition and anti-quorum sensing activity of phytosynthesized silver nanoparticles against the nosocomial pathogen *Pseudomonas aeruginosa*, Biofouling. 35 (2019) 34–49. https://doi.org/10.1080/08927014.2018.1563686.
28. P. Singh, S. Pandit, J. Garnæs, S. Tunjic, V. Mokkapati, A. Sultan, A. Thygesen, A. Mackevica, R.V. Mateiu, A.E. Daugaard, A. Baun, I. Mijakovic, Green synthesis of gold and silver nanoparticles from Cannabis sativa (industrial hemp) and their capacity for biofilm inhibition, Int J Nanomedicine. Volume 13 (2018) 3571–3591. https://doi.org/10.2147/IJN.S157958.
29. S. Liao, Y. Zhang, X. Pan, F. Zhu, C. Jiang, Q. Liu, Z. Cheng, G. Dai, G. Wu, L. Wang, L. Chen, Antibacterial activity and mechanism of silver nanoparticles against multidrug-resistant Pseudomonas aeruginosa, Int J Nanomedicine. Volume 14 (2019) 1469–1487. https://doi.org/10.2147/IJN.S191340.
30. S. Tang, J. Zheng, Antibacterial Activity of Silver Nanoparticles: Structural Effects, Adv Healthc Mater. 7 (2018) 1701503. https://doi.org/10.1002/adhm.201701503.

Preprints (www.preprints.org) | NOT PEER-REVIEWED | Posted: 5 June 2023 doi:10.20944/preprints202306.0308.v1

31. T.C. Dakal, A. Kumar, R.S. Majumdar, V. Yadav, Mechanistic Basis of Antimicrobial Actions of Silver Nanoparticles, Front Microbiol. 7 (2016). https://doi.org/10.3389/fmicb.2016.01831.
32. A. Mandal, S. Sekar, N. Chandrasekaran, A. Mukherjee, T.P. Sastry, Synthesis, characterization and evaluation of collagen scaffolds crosslinked with aminosilane functionalized silver nanoparticles: in vitro and in vivo studies, J Mater Chem B. 3 (2015) 3032–3043. https://doi.org/10.1039/C4TB02124J.
33. M.J. Kühn, L. Talà, Y.F. Inclan, R. Patino, X. Pierrat, I. Vos, Z. Al-Mayyah, H. Macmillan, J. Negrete, J.N. Engel, A. Persat, Mechanotaxis directs Pseudomonas aeruginosa twitching motility, Proceedings of the National Academy of Sciences. 118 (2021). https://doi.org/10.1073/pnas.2101759118.
34. A. Travan, C. Pelillo, I. Donati, E. Marsich, M. Benincasa, T. Scarpa, S. Semeraro, G. Turco, R. Gennaro, S. Paoletti, Non-cytotoxic Silver Nanoparticle-Polysaccharide Nanocomposites with Antimicrobial Activity, Biomacromolecules. 10 (2009) 1429–1435. https://doi.org/10.1021/bm900039x.
35. N. Amiri, S. Ajami, A. Shahroodi, N. Jannatabadi, S. Amiri Darban, B.S. Fazly Bazzaz, E. Pishavar, F. Kalalinia, J. Movaffagh, Teicoplanin-loaded chitosan-PEO nanofibers for local antibiotic delivery and wound healing, Int J Biol Macromol. 162 (2020) 645–656. https://doi.org/10.1016/j.ijbiomac.2020.06.195.
36. C. Tyavambiza, M. Meyer, S. Meyer, Cellular and Molecular Events of Wound Healing and the Potential of Silver Based Nanoformulations as Wound Healing Agents, Bioengineering. 9 (2022) 712. https://doi.org/10.3390/bioengineering9110712.
37. X. Liu, P. Lee, C. Ho, V.C.H. Lui, Y. Chen, C. Che, P.K.H. Tam, K.K.Y. Wong, Silver Nanoparticles Mediate Differential Responses in Keratinocytes and Fibroblasts during Skin Wound Healing, ChemMedChem. 5 (2010) 468–475. https://doi.org/10.1002/cmdc.200900502.
38. K. Zhang, V.C.H. Lui, Y. Chen, C.N. Lok, K.K.Y. Wong, Delayed application of silver nanoparticles reveals the role of early inflammation in burn wound healing, Sci Rep. 10 (2020) 6338. https://doi.org/10.1038/s41598-020-63464-z.

Disclaimer/Publisher's Note: The statements, opinions and data contained in all publications are solely those of the individual author(s) and contributor(s) and not of MDPI and/or the editor(s). MDPI and/or the editor(s) disclaim responsibility for any injury to people or property resulting from any ideas, methods, instructions or products referred to in the content.